MoS_2 Field-Effect Transistors With Graphene/Metal Heterocontacts

Yuchen Du, Lingming Yang, Jingyun Zhang, Han Liu, Kausik Majumdar,
Paul D. Kirsch, and Peide D. Ye, *Fellow, IEEE*

***Abstract*— For the first time, n-type few-layer MoS_2 field-effect transistors (FETs) with graphene/Ti as the heterocontacts have been fabricated, showing more than 160-mA/mm drain current at 1-μm gate length with an ON-OFF current ratio of 10^7. The enhanced electrical characteristic is confirmed in a nearly 2.1 times improvement in ON-resistance and a 3.3 times improvement in contact resistance with heterocontacts compared with the MoS_2 FETs without graphene contact layer. Temperature-dependent study on MoS_2/graphene heterocontacts has been also performed, still unveiling its Schottky contact nature. Transfer length method and a devised *I–V* method have been introduced to study the contact resistance and Schottky barrier height in MoS_2/graphene/metal heterocontacts structure.**

***Index Terms*— MoS_2, graphene, heterocontacts, MOSFET, Schottky barrier height.**

I. Introduction

Graphene and other two-dimensional (2D) materials are the rapidly rising stars on the horizon of materials science, condensed-matter physics, and solid state devices. They stand for a brand new family of materials that are one or few atomic layer thick, and offer many new research directions towards nanoscience and nanotechnology. However, the gapless nature of monolayer graphene has restrained its wide electronic device applications, in particularly for logic circuits [1]. Transition metal dichalcogenides (TMDs), another type of 2D materials, recently attracted wide attentions due to their appropriate bandgap and reasonable mobility. Owing to its unique structural and electronic properties, TMDs provide us novel material systems to explore interesting phenomena, such as 2D interfaces, which might be not available to be investigated in the traditional Si and III-V semiconductors. As one of the most studied TMDs, MoS_2 has a bandgap between 1.3-1.8 eV, depending on the number of layers, and reasonable mobility [2], [3]. The on-state performance of the MoS_2 FETs is mainly limited by the large contact resistance at MoS_2/metal interfaces [4]–[9]. Recent attempts to improve MoS_2 contacts had been concentrated on the following areas using: (1) low work function contact metal [10], (2) gas doping of MoS_2 flakes [11], and (3) molecular or solid doping on MoS_2 films [12], [13]. However, the fundamental reason for the large contact resistance is the result of Fermi level pinning on MoS_2 near conduction band edge due to S-vacancy defect level and charge neutral level location [14], [15]. All above experiments have just partially touched the issue and barely resolved the issue completely. Graphene contacts on MoS_2 [9], which has a 2D to 2D interface, might provide a new angle to solve this technical challenge. In this letter, graphene is used in between metal contact and n-type few-layer MoS_2 film to enhance the electronic coupling between metal and MoS_2 and boost the electron injection into MoS_2. For the first time, well-performed graphene/metal hetero-contacts MoS_2 FETs were fabricated. The feasibility using graphene/ metal hetero-contacts to reduce contact resistance (R_c) and improve on-resistance (R_{on}) of the devices is demonstrated.

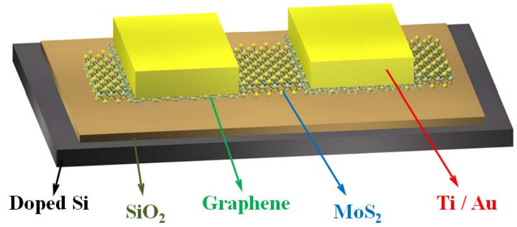

Fig. 1. Structure geometry of hetero-contacts MoS_2/Graphene/Metal FETs with a channel length of 1 μm.

II. Experiment

MoS_2 flakes with 5-6nm thickness were mechanically exfoliated from bulk ingot (SI Supplies) by standard scotch tape technique, and then transferred to a heavily p-doped silicon substrate with a 90 nm SiO_2 capping layer. Monolayer CVD graphene grown on Cu foil (Graphene Supermarket Inc.) was transferred onto the MoS_2/SiO_2/Si wafer with the PMMA method: A 500 nm PMMA (10% in Anisole) layer was first spin-coated on graphene/Cu. The copper substrate was etched using 1M $FeCl_3$ solution. After rinsing in DI water for several times, the PMMA/graphene layer was transferred onto the target substrate. The sample was dried in N_2 ambient for 12 hours, and then PMMA was removed by rinsing in acetone bath. An additional H_2/N_2 annealing at 450 °C was used to remove the PMMA residues. After the graphene film transfer onto the MoS_2/SiO_2/Si substrate, electron beam lithography was used to pattern the source and drain contacts, combining with low power oxygen etch to isolate the source/drain, and the different devices. Graphene is fully etched from the channel. Metallization was performed by electron-beam evaporation of 20 nm/60 nm Ti/Au with the size 50 nm smaller at each side

Manuscript received February 28, 2014; revised March 19, 2014; accepted March 20, 2014. Date of publication April 4, 2014; date of current version April 22, 2014. This work was supported in part by SEMATECH and in part by SRC under Tasks 2362 and 2396. The review of this letter was arranged by Editor K. Uchida.

Y. Du, L. Yang, J. Zhang, H. Liu, and P. D. Ye are with the Birck Nanotechnology Center, School of Electrical and Computer Engineering, Purdue University, West Lafayette, IN 47907 USA (e-mail: yep@purdue.edu).

K. Majumdar and P. D. Kirsch are with SEMATECH, Albany, NY 12203 USA.

Color versions of one or more of the figures in this letter are available online at http://ieeexplore.ieee.org.

Digital Object Identifier 10.1109/LED.2014.2313340

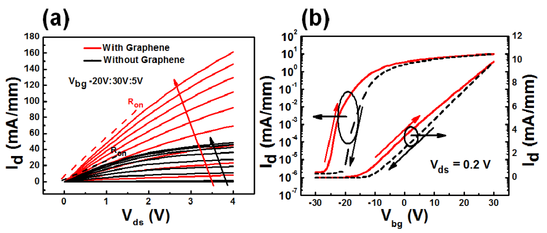

Fig. 2. (a) Output curve of FETs with and without graphene contacts. The backgate voltage sweeps from -20 V to 30 V with a step of 5 V. (b) Transfer curve of the hetero-contacts FETs in log (left) and linear (right) scale. Both forward (solid) and backward (dash) sweeps are shown.

than graphene contacts as illustrated in Fig. 1. In order to have accurate comparison, similar device without monolayer graphene were also fabricated on few-layer MoS_2 with a similar thickness and the same channel length. Electrical measurements were carried out with Keithley 4200 semiconductor parameter analyzer and probe station in ambient atmosphere.

III. Results and Discussion

Output and transfer curves of a hetero-contacts FET are plotted in Fig. 2(a) and (b) to demonstrate its effectiveness to improve device performance by inserting monolayer graphene between metal and MoS_2 contacts. The output curves of a reference sample are also shown in Fig. 2(a) in black. For the device contact without graphene, shown in Fig. 2(a), on-current at $V_{ds} = 4$ V, and $V_{bg} = 30$ V is equal to 48.5 mA/mm. As the monolayer graphene applied in the hetero-contacts, on-current is improved to be 161.2 mA/mm at the same source/drain and gate bias. R_{on} determined from linear region as shown in Fig. 2(a) as dashed lines are used to have a direct comparison. Comparing to R_{on} of 42.8 Ω·mm for the reference device, hetero-contacts device shows a much lower R_{on} of 20.6 Ω·mm. In order to have a more accurate comparison, metal contacts with and without graphene on the same flake have also been fabricated. Similar values of R_{on} and similar amount of reduction in R_{on} have been achieved. The results further verified the feasibility of using graphene/metal hetero-contacts to improve on-resistance of the devices. With similar channel resistance of two devices, the nearly 2.1 times dropping in R_{on} is directly related to the reduction of R_c by inserting monolayer of graphene into contact. In Fig. 2(b), the transfer curves of hetero-contacts FETs are plotted with source/drain biases of 0.2 V. The exhibiting hysteresis from forward and backward sweeps is due to the charge injection at the interface between MoS_2 and the substrate and the charge transfer from/to neighboring adsorbates [16]. The 10^7 current on/off ratio is achieved on hetero-contacts devices. Extrinsic field-effect mobility of hetero-contacts FETs is calculated to be 32.3 cm^2/Vs, which is extracted from the forward I-V transfer curves by the relation,

$$\mu = \frac{dI_{ds}}{d(V_{bg})} \times \frac{L}{w \times C_{ox} \times V_{ds}} \quad (1)$$

where $\frac{dI_{ds}}{d(V_{bg})}$ is the transconductance, L is the channel length, W is the channel width, and C_{ox} is the backgate capacitance per unit area. Using R_c of hetero-contacts device ~3.7 Ω·mm, intrinsic field-effect mobility of 50.4 cm^2/Vs is obtained.

A devised I-V method has been used to quantitatively investigate the Schottky barrier height of hetero-contacts of MoS_2/graphene/metal [17]. The barrier height is calculated from the current I_s, determined by extrapolating the semilog I_d versus V_d curve to V_d =0 V. Schottky barrier height I_s is calculated from I_s according to

$$\phi_B = \frac{K_B T}{q} \text{In}(\frac{A \times A^* \times T^2}{I_s}) \quad (2)$$

where A is the area, A* is the Richardson constant, and T is the temperature. Due to the uncertainty of A* [17], the effective Schottky barrier height cannot be accurately calculated directly, however, instead of calculating the exact value of Schottky barrier height, exponential function of barrier height can be readdressed. Normalized exponential Schottky barrier height versus backgate voltage has been plotted in Fig. 3(a) to demonstrate the Schottky barrier deduction with graphene contact. Moreover, transfer length method (TLM) with separations of 0.5 μm, 1 μm, 1.5 μm, and 2 μm are used to accurately extract the contact resistance of MoS_2/graphene/metal hetero-contacts. Contact resistance without graphene has also been extracted by applying TLM structure on a similar thickness flake. In Fig. 3, both Schottky barrier and contact resistance show a strong gate bias dependent behavior. It is because (1) gate-tunable Schottky barrier width reduction due to the increment of backgate bias and (2) carrier concentration enhancement from backgate bias doping, where all lead to reduce the effective Schottky barrier height and generate more injected electrons from Fermi level at metal to conduction band of MoS_2. To exclude the large absolute errors, high bias regions are appropriate to have direct comparison in the contact resistance. Contact resistance with monolayer graphene is 3.7±0.3 Ω·mm at $V_{bg} = 30$ V, which decreased from a value of 12.1±1.2 Ω·mm at the same backgate voltage without the graphene layer. This nearly 3.3 times reduction in contact resistance may possibly be attributed to the gate-induced electron injection from graphene layer to MoS_2. At the hetero-contact structure, the positive back-gate bias not only electro-statically dopes MoS_2, but also could move the Fermi-level in Ti doped n-type graphene [18]–[21] further up beyond the Ti/MoS_2 pinning level, thus enhance the electron injection from metal into the conduction band of MoS_2 leading to a lower contact resistance. The key difference from previous devices is that the back-gate can modulate not only the Fermi-level of the channel but also the contact (graphene) as shown in the inset of Fig. 3(b) [19]. The total carrier density summed over graphene and MoS_2 hetero-contact exceeds the single MoS_2/metal contact, where the monolayer graphene can be seemed as a "charge pumping" layer. It seems that 2D graphene to MoS_2 interface is fundamentally different from metals to MoS_2 interfaces.

Temperature dependent measurements of graphene/metal contact on MoS_2 have been also performed. Substrate temperatures are changed from 300 K to 400 K, and the electrical transport properties are reported in Fig. 4. As the temperature goes up, thermal-assistant tunneling improves the electron injection efficiency from the hetero-contacts to MoS_2 channel through the Schottky barrier, thus lowering the

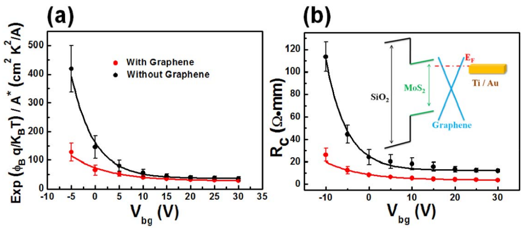

Fig. 3. (a) Normalized exponential Schottky barrier height versus back-gate voltage (b) Contact resistance versus back-gate voltage for both contact with graphene and contact without graphene. Inset: Schematic band diagram of a metal/graphene/MoS_2 hetero-contact at a very positive gate bias with a zero drain bias. Error bars are determined from the standard errors of the linear fitting under different back-gate biases.

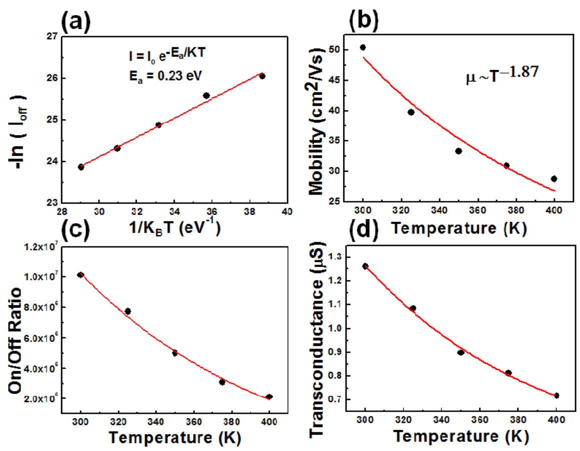

Fig. 4. Temperature dependent measurement from 300 K to 400 K on (a) Off state current, (b) Intrinsic mobility, (c) On/off ratio, (d) Transconductance.

contact resistance. Meanwhile, higher temperature also causes off-current I_{off} to increase rapidly, where insulating behavior in off-state well fits to the activated temperature-dependent current. Calculated activation energy of MoS_2, $E_a = 0.23$ eV, is the slope of Arrhenius plot in Fig. 4(a). The thermal activity involved off-state conducting has the energy that is smaller than the band gap of MoS_2, which may correspond to the depth of the donor levels [22], [23] most likely caused by natural material defects [14], [15]. As depicted in Fig. 4(c), the current on/off ratio drops with the increase of temperature, because of the increment of off-state current. Intrinsic field-effect mobility has been extracted in Fig. 4(b). In the range of 300 K to 400 K, the temperature dependent intrinsic field-effect mobility is decreased from 50.4 cm^2/Vs at 300 K to the lowest value of 28.7 cm^2/Vs at 400K due to the electron-phonon scattering. Temperature dependence of the mobility follows the equation $\mu \sim T^{-\upsilon}$, where the exponent υ depends on the dominating phonon scattering mechanism. From the generic temperature dependence fitting curve, we find the value of υ equals 1.87, which is larger than the value of 1.4-1.6 obtained from MoS_2 temperature dependent Hall mobility measurement [23], [24]. The discrepancy could be related to the behavior of traps which affects field-effect mobility much more [25], [26].

IV. Conclusion

In summary, we have demonstrated the first MoS_2 field-effect transistor with graphene/metal hetero-contacts. Graphene hetero-contacts effectively reduce the contact resistance from 12.1±1.2 Ω·mm to 3.7±0.3 Ω·mm, compared to the reference MoS_2/metal contacts. The nearly 3.3 times improvement in R_c is attributed to the gate-enhanced electron injection from metal doped n-type graphene into MoS_2 conduction band, which provides a new route to engineer 2D contacts towards the realization of Ohmic contacts on MoS_2 and other 2D materials.

References

[1] Y. Q. Wu *et al.*, "High-frequency, scaled graphene transistors on diamond-like carbon," *Nature*, vol. 472, no. 7341, pp. 74–78, 2011.
[2] K. F. Mak *et al.*, "Atomically thin MoS_2: A new direct-gap semiconductor," *Phys. Rev. Lett.*, vol. 105, no. 13, p. 136805, 2010.
[3] B. Radisavljevic *et al.*, "Single-layer MoS_2 transistors," *Nat. Nanotechnol.*, vol. 6, no. 3, pp. 147–150, 2011.
[4] W. Bao *et al.*, "High mobility ambipolar MoS_2 field-effect transistors: Substrate and dielectric effects," *Appl. Phys. Lett.*, vol. 102, no. 4, pp. 042104-1–042104-4, 2013.
[5] Y. Yoon, K. Ganapathi, and S. Salahuddin, "How good can monolayer MoS_2 transistors be," *Nano Lett.*, vol. 11, no. 9, pp. 3768–3773, 2011.
[6] F. K. Perkins *et al.*, "Chemical vapor sensing with monolayer MoS_2," *Nano Lett.*, vol. 13, no. 2, pp. 668–673, 2013.
[7] Z. Y. Yin *et al.*, "Single-layer MoS_2 phototransistors," *ACS Nano*, vol. 6, no. 1, pp. 74–80, 2012.
[8] H. Wang *et al.*, "Integrated circuits based on bilayer MoS_2 transistors," *Nano Lett.*, vol. 12, no. 9, pp. 4674–4680, 2012.
[9] J. Yoon *et al.*, "Highly flexible and transparent multilayer MoS_2 transistors with graphene electrodes," *Small*, vol. 9, no. 19, pp. 3295–3300, 2013.
[10] S. Das *et al.*, "High performance multilayer MoS_2 transistors with scandium contacts," *Nano Lett.*, vol. 13, no. 1, pp. 100–105, 2013.
[11] H. Fang *et al.*, "Degenerate n-doping of few-layer transition metal dichalcogendies by potassium," *Nano Lett.*, vol. 13, no. 5, pp. 1991–1995, 2013.
[12] Y. C. Du *et al.*, "Molecular doping of multilayer MoS_2 field-effect transistors: Reduction in sheet and contact resistances," *IEEE Electron Device Lett.*, vol. 34, no. 10, pp. 1328–1330, Oct. 2013.
[13] M. R. Laskar *et al.*, "P-type doping of MoS_2 thin films using Nb," *Appl. Phys. Lett.*, vol. 104, no. 9, p. 092104, 2014.
[14] C. Gong *et al.*, "Metal contacts on physical vapor deposited monolayer MoS_2," *ACS Nano*, vol. 7, no. 12, pp. 11350–11357, 2013.
[15] D. Liu *et al.*, "Sulfur vacancies in monolayer MoS_2 and its electrical contacts," *Appl. Phys. Lett.*, vol. 103, no. 18, pp. 183113-1–183113-4, 2013.
[16] D. J. Late *et al.*, "Hysteresis in single-layer MoS_2 field effect transistors," *ACS Nano*, vol. 6, no. 6, pp. 5635–5641, 2012.
[17] D. K. Schroder, *Semiconductor Material and Device Characterization*, 3rd ed. New York, NY, USA: Wiley, 2006.
[18] G. Giovannetti *et al.*, "Doping graphene with metal contacts," *Phys. Rev. Lett*, vol. 101, no. 2, p. 026803, 2008.
[19] S. Larentis *et al.*, "Band offset and negative compressibility in graphene-MoS_2 heterostructures," *Nano Lett.*, to be published.
[20] J. A. Robinson "Contacting graphene," *Appl. Phys. Lett.*, vol. 98, no. 5, p. 053103, 2011.
[21] K. Pi *et al.*, "Electronic doping and scattering by transition metals on graphene," *Phys. Rev. B*, vol. 80, no. 7, p. 075406, 2009.
[22] J. Pu *et al.*, "Highly flexible MoS_2 thin-film transistors with ion gel dielectrics," *Nano Lett.*, vol. 12, no. 8, pp. 4013–4017, 2012.
[23] A. T. Neal *et al.*, "Magneto-transport in MoS_2: Phase coherence, spin-orbit scattering, and the Hall factor," *ACS Nano*, vol. 7, no. 8, pp. 7077–7082, 2013.
[24] B. Radisavljevic and A. Kis, "Mobility engineering and a metal-insulator transition in monolayer MoS_2," *Nat. Mater.*, vol. 12, pp. 815–820, Jan. 2013.
[25] H. Qiu *et al.*, "Hopping transport through defect-induced localized states in molybdenum disulphide," *Nature Commun.*, vol. 4, p. 2642, Sep. 2013.
[26] W. Zhu *et al.*, "Electronic transport and device prospects of monolayer molybdenum disulphide grown by chemical vapour deposition," *Nature Commun.*, vol. 5, p. 3087, Jan. 2014.